A Viscous Isolator for Shuttle Hubble Space Telescope Resupply

by
Porter Davis,
Frank Schmitt, and Charles See

Honeywell Inc.
Satellite Systems Divsion
19019 N. 59th Avenue
Glendale, Arizona 85308
(602) 561-3000

ABSTRACT

Two isolator designs are being developed using the Hubble Space Telescope (HST) Reaction Wheel Assembly (RWA) isolator heritage. The first application provides a six-degree-of-freedom passive isolation system for space shuttle payloads. The HST solar arrays and science instrument packages cannot survive launch and reentry when directly exposed to shuttle vibration. The isolation mount for these payloads consists of a carrier assembly attached to the shuttle structure by an array of isolator struts. Various isolation characteristics, obtained by varying the strut's spring arrangement and damping coefficient, were evaluated. Twelve identical struts are arranged in tripods at each of the four corners of the carrier for redundancy and isoelasticity. The entire isolated mass has its resonance at 8 Hz with a damping ratio of 0.4; the effective loading is reduced by at least a factor of two. Prototype isolators have been built and characterization has been done. This provides the basis for the flight design currently underway.

The second application is to provide isolation between the Space Station and the Payload Pointing System. An array of struts, each containing damping and spring elements, was studied. The requirement for the first mode to be significantly lower than 0.05 Hz necessitates the use of novel approaches to design very soft springs.

INTRODUCTION

There is an increasing need for vibration isolation for spacecraft applications. Two specific applications of isolation technology are: 1) to reduce emitted vibrations from dynamic hardware, such as rotating machinery, and 2) to protect sensitive hardware from launch vibration and spacecraft disturbances. The Hubble Space Telescope (HST) Reaction Wheel Assembly (RWA) Isolator (Figure 1) is an example of the first application. It significantly reduces the vibrations emitted from the RWA, which would limit the telescopes imaging ability (Figure 2). Such isolation is also important to sensitive pointing systems and mircrogravity research and processing.

Two isolator designs are being developed using the HST-RWA isolator heritage for the second application, that of hardware isolation. The HST-Solar Array System Isolator (SASI) provides six-degree-of-freedom (DOF) passive isolation for space shuttle payloads. The Payload Pointing System (PPS) isolator provides isolation between the Space Station and the Payload Pointing System, which requires a first mode significantly lower than 0.05 Hz.

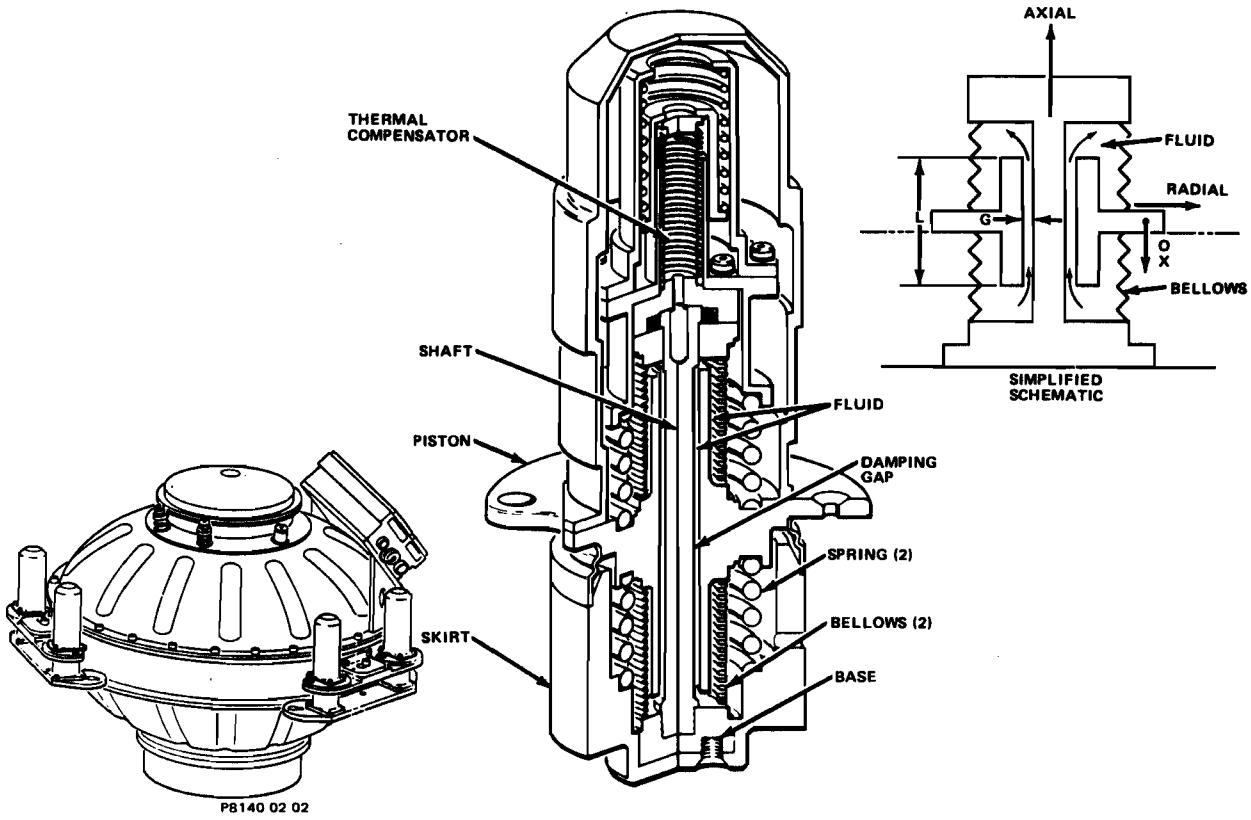

Figure 1. Hubble Space Telescope RWA Heritage

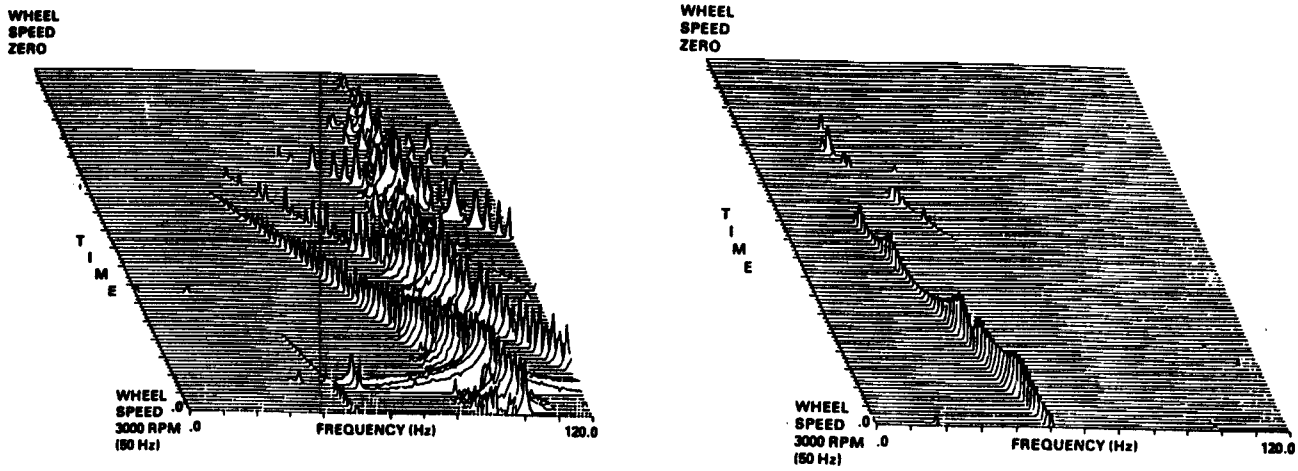

Hard-Mounted Reaction Wheel Axial Force (3.39 lb Peak)

Isolated (Honeywell Viscous Isolator) Reaction Wheel Axial Force (0.025 lb Peak)

Figure 2. RWA Disturbance Isolation

THE HST-SOLAR ARRAY SYSTEM ISOLATOR (SASI)

The significantly large mass of the HST satellite causes its first mode of vibration to be relatively low while mounted in the space shuttle cargo bay. Consequently, the vibration spectra seen by hardware attached to it, such as the solar arrays and axial scientific instruments, are attenuated for frequencies substantially above this mode. When considering resupply of these items to the HST vehicle, it is necessary to assure that launch vibrations experienced do not exceed the design capabilities. Consequently, it is necessary to isolate these items from the shuttle.

The Solar Array (SA) Carrier (Figure 3) provides the needed isolation for the SAs by using twelve spring-damper isolations elements configured in four tripods. The carrier attaches to the shuttle via a removable/jettisonable deck. The tripod arrangement, as presented in Figure 4, is configured to provide iso-elastic isolation and failsafe redundancy at each attachment point. The effect of this isolation system is presented in Figure 5. Unisolated, the response spectrum produces stresses in the solar arrays in excess of their design limits. This spectrum consists primarily of high-frequency components. Isolating the carrier with spring elements tuned to significantly lower frequency, in this case, 8 Hz, substantially reduces the higher frequency response. However, the spring elements introduce a response peak at the resonant frequency. Introducing damping limits the resonant peaking and produces a substantially reduced response spectrum. The result is induced stresses within the design limits of the solar arrays.

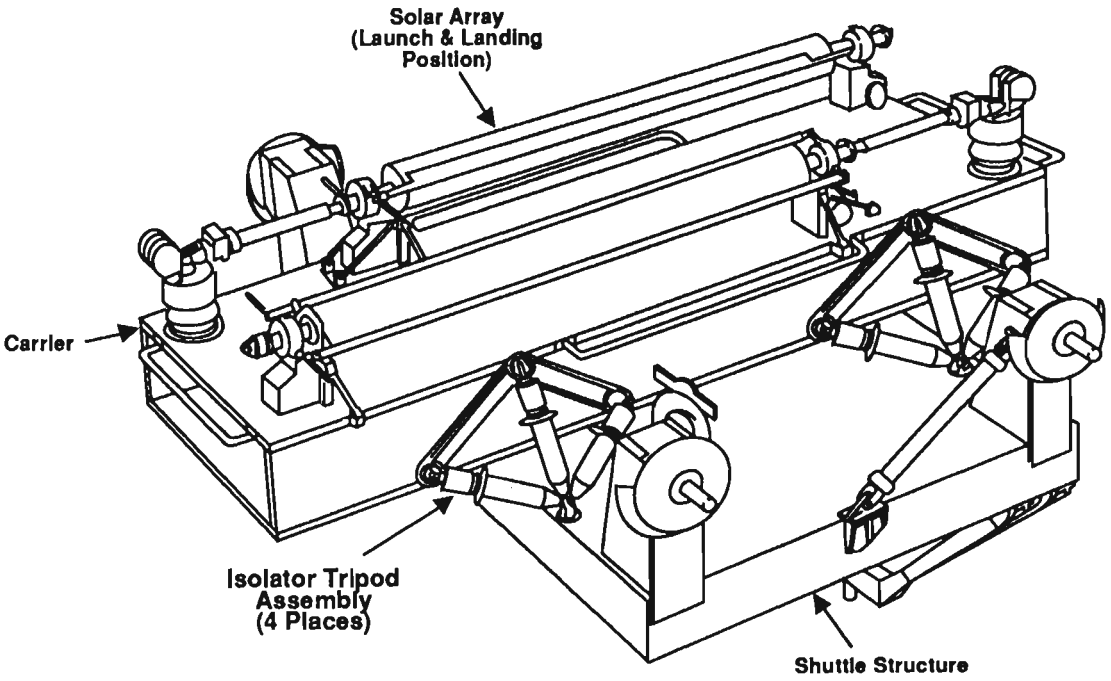

Figure 3. Isolated Solar Array Carrier

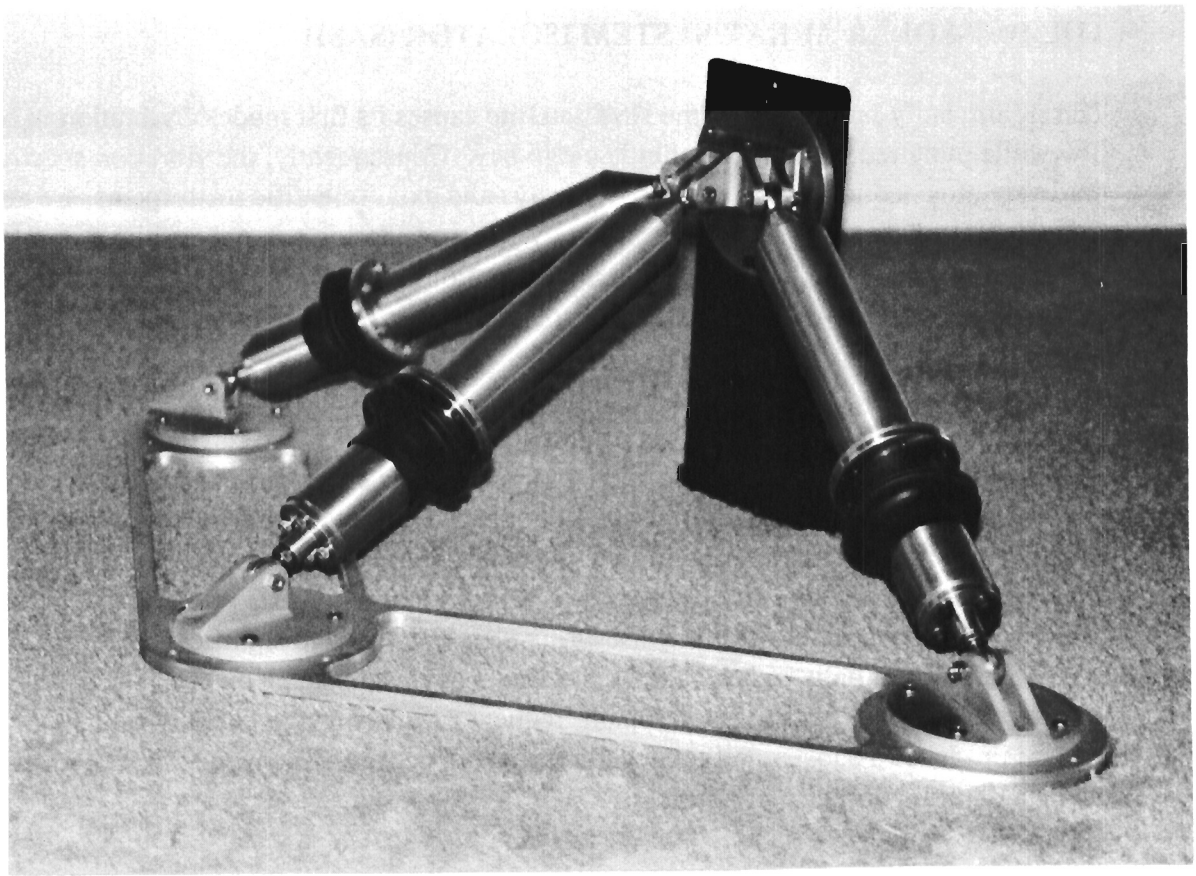

Figure 4. SASI Tripod Arrangement

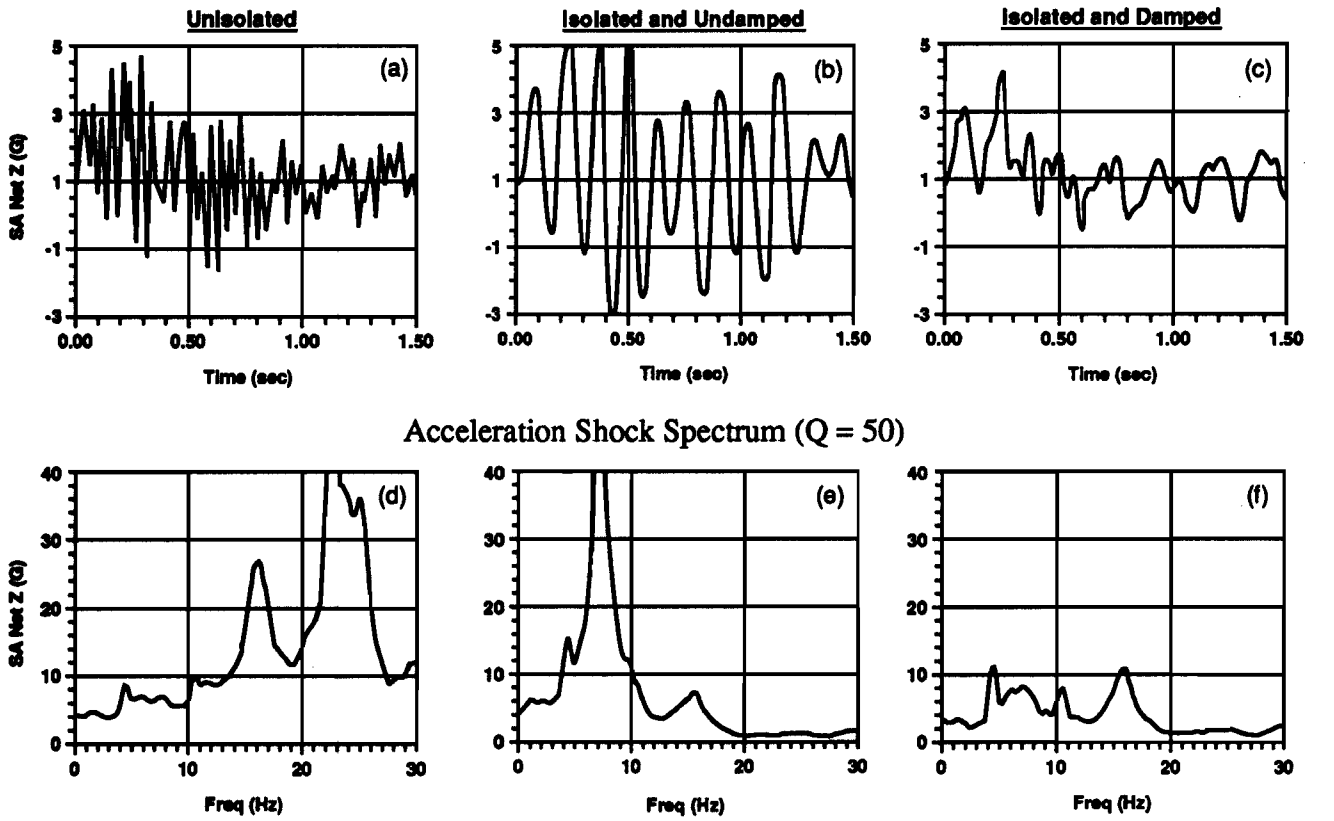

Courtesy of Bill Haile, Swales and Associates, Beltsville, MD

Figure 5. Representative Solar Array Response Changes

To verify manufacture isolator element performance against the characteristics of those in the analytical model, prototype isolator elements were designed, built, and tested to the specifications presented in Table 1. The prototype elements presented in Figures 6 and 7 provide passive damping via a viscous silicon fluid that is forced through an annular passage between two bellows-type pressure chambers. As the isolator is exercised, the volume of one of the chambers is increased at the same rate as the other is decreased, resulting in consistent damping. A compensation device provides for thermal expansion of the fluid and preloads the chambers to avoid cavitation. Helically wound coil springs are used to provide the correct stiffness for isolation.

Two types of dynamic tests were run on the prototype isolators: a transmissibility transfer function test and a velocity/pressure margin test. The transfer function test, as shown in Figure 8, consisted of connecting the isolator element between a suspended mass and an electromagnetic shaker. The mass was sized to provide an 8-Hz resonant frequency. The shaker was swept at a constant acceleration from approximately 4 to 200 Hz. Accelerometers on the shaker and mass were used to plot the transfer function, from which the Q and damping coefficients were calculated. The test was run for two different viscosity fluids: 250 centistoke and 500 centistoke. The results are presented in Figure 9.

Table 1. SASI Prototype Element Specification

Deflection	±0.5 in.
Velocity	11.5 in./s
Damping	2.6 lb-s/in.
Stiffness	400 lb/in.
Temperature	
Design	14°C to 36°C
Storage	-25°C to +40°C
Length	15 in.
Diameter	3 in.
Weight	≈ 3 lb

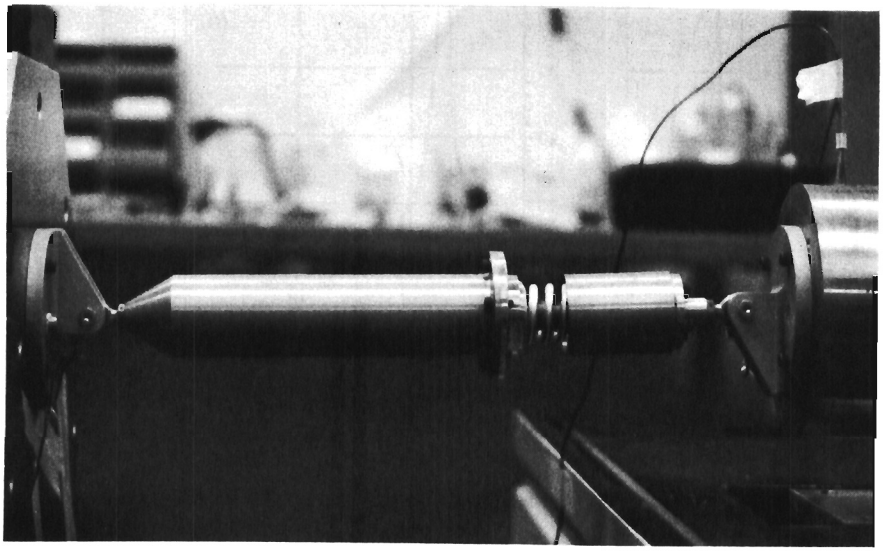

Figure 6. SASI Prototype

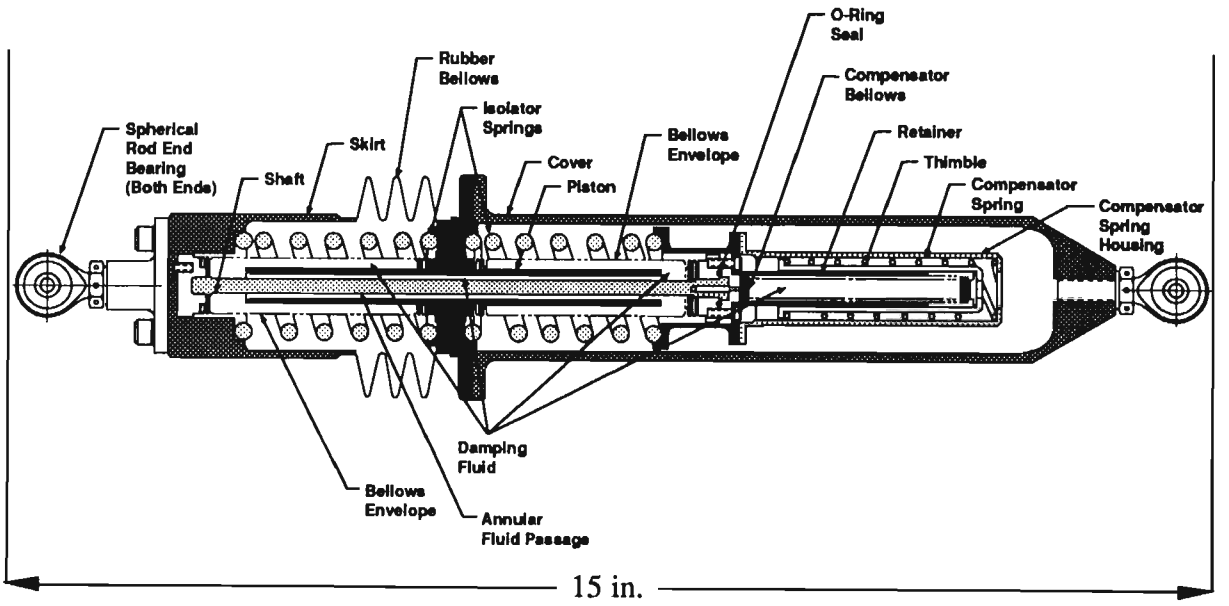

Figure 7. SASI Prototype Element

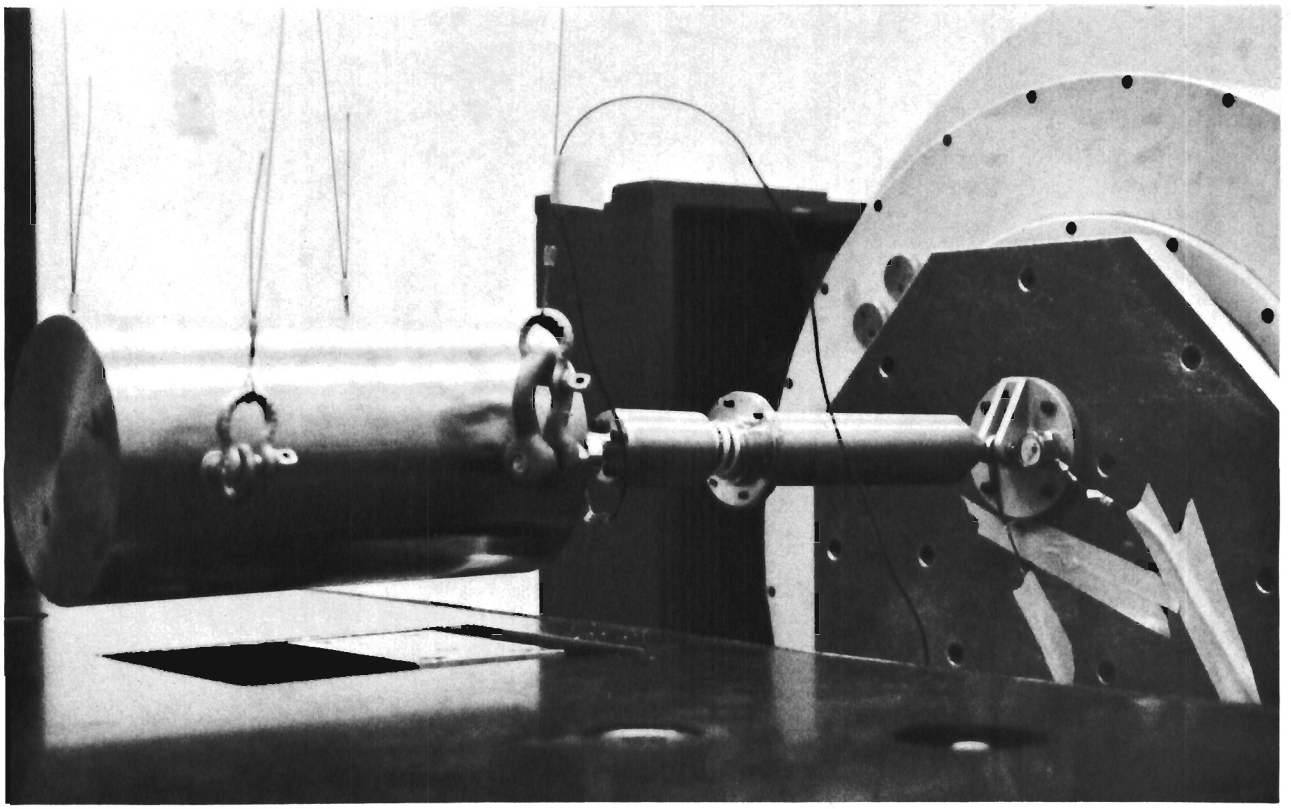

Figure 8. Transfer Function

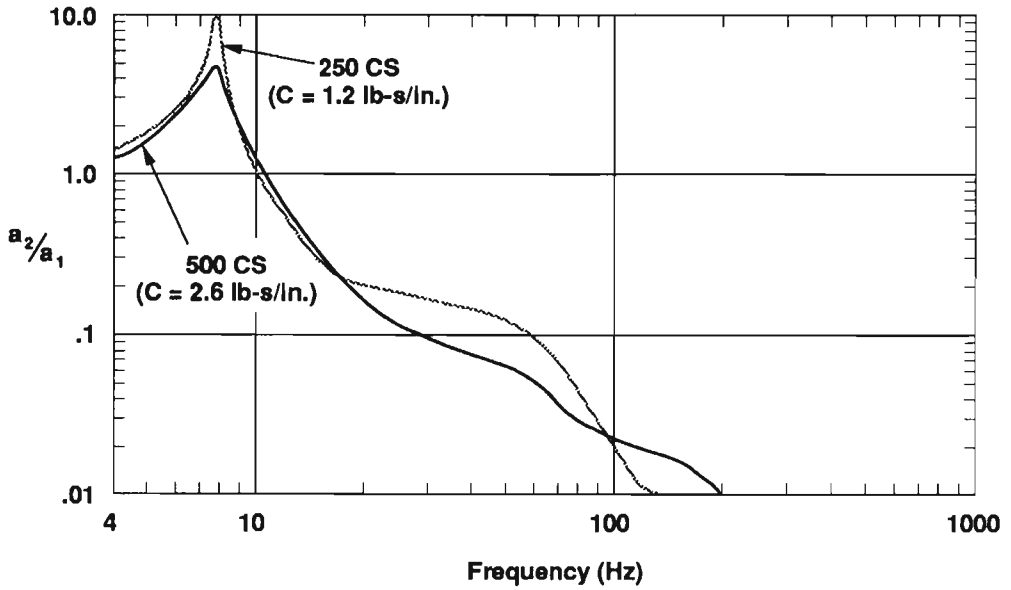

Figure 9. Transfer Function Test Results

Verification of the damper design was accomplished by rigidly fixing one end of the isolator to the shaker frame and driving the other end at a constant amplitude displacement, as shown in Figure 10. The frequency of excitation was swept to provide velocities from below nominal to those that produced chamber pressures equal to the bellows-proof pressure.

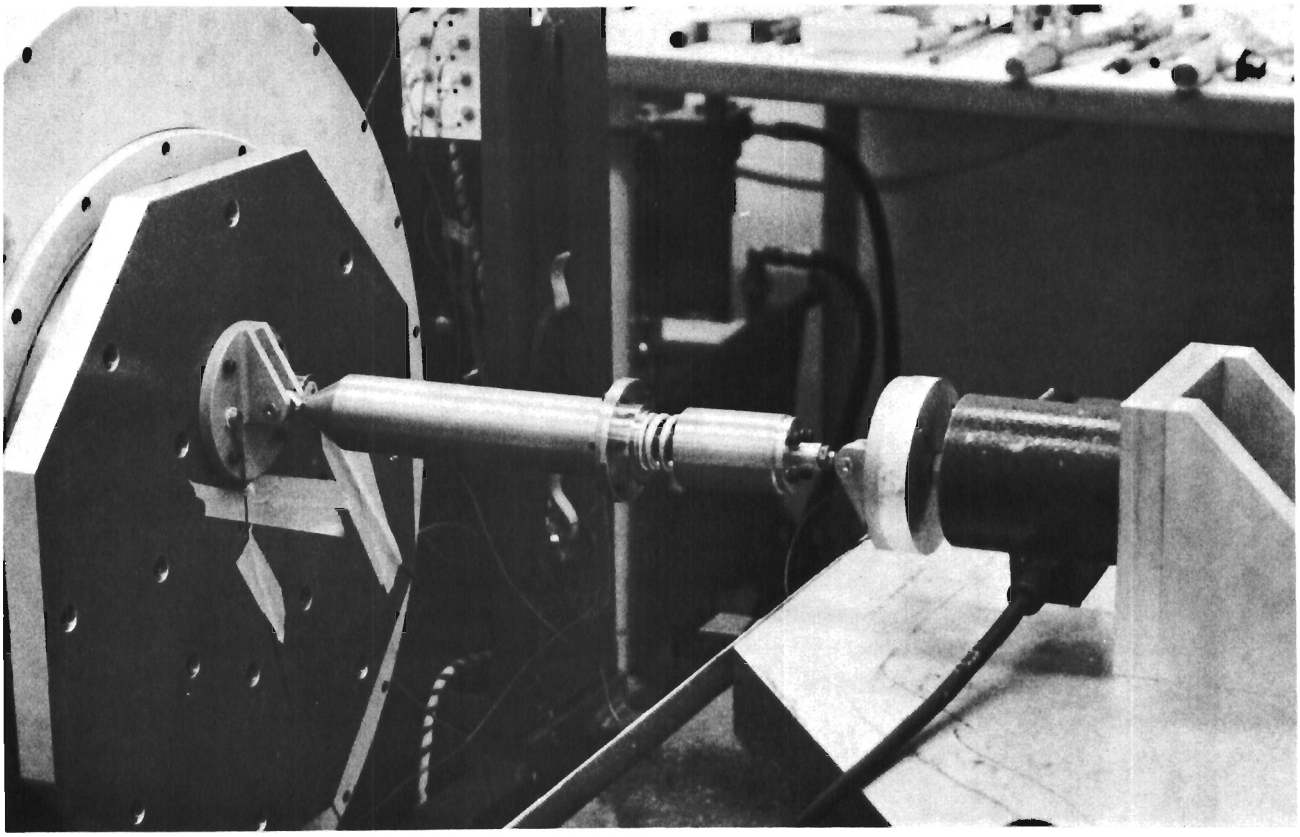

Figure 10. Velocity Test

The storage temperature range was demonstrated by thermal cycling the prototype and rerunning the transfer function test. The stiffness, stroke, and weight were measured during assembly. A summary of the prototype test results is presented in Table 2. Off-the-shelf springs were used to decrease procurement time; consequently, their stiffness did not match the design goal. Variation in spring length and stiffness resulted in asymmetric assembly, causing less usable stroke to be available than was originally desired. With these exceptions, the prototypes behaved very much as expected.

Table 2. Prototype Test Summary

	Design Goal	Test Results (500 cs)
Stiffness (lb/in.)	400	570
Damping (lb-s/in.)	2.6	2.6
Resonance (Hz)	8.0	7.8
Stroke (in.)	±0.5	±0.44
Weight (lb)	≈ 3.0	3.02
Velocity Capacity (in./s)	11.5	41.5
Storage Temperature (°C)	-25 to +40	-25 to +40

The actual isolation requirements for the solar array carrier necessitate isolator elements that are considerably larger than those used for prototype testing (Figure 11). The flight isolator design requirements are presented in Table 3. The higher peak velocity requirements necessitate extremely large bellows in order to keep the chamber pressure within the design limits. The increased stroke requirements also drive the bellows' size up, due to increased fatigue loading.

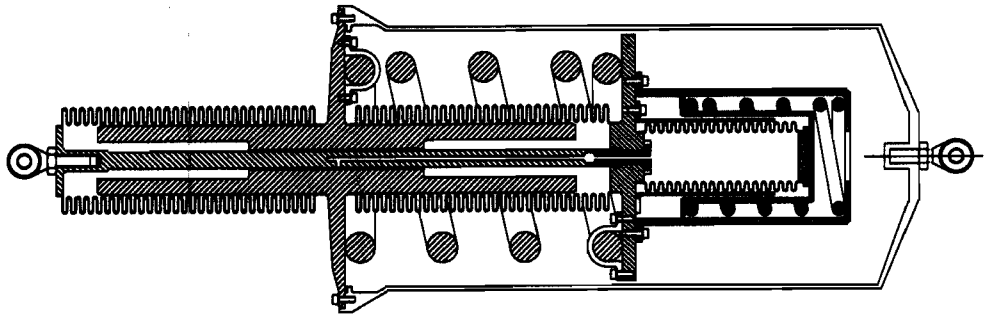

Figure 11. SASI Bellows-Type Isolator Element

Table 3. Isolator Element Flight Specification

Deflection	±0.91 in.
Velocity	±15 in./s
Damping	35 lb-s/in.
Stiffness	1875 lb/in.
Temperature	
Design	25 ± 5°C
Storage	-35°C to +49°C
Length	27 in. Brg ℄ to Brg ℄
Body Diameter	8 in. max
Fatigue Life	10,000 full stroke cycles
Weight	33 lb

To combat the increased size and weight, a higher pressure capacity damper (originally designed for isolation from Titan launch loads) was adapted to the isolator (Figure 12). It operates on the same principal of viscous flow through an annular gap to provide damping, but can withstand much higher internal pressures. Small displacement performance is sacrificed, however due to stiction in the O-ring seals. The parameters used in the design of the isolators presented in Figure 12 are listed in Table 4. A metal bellows could be added to provide a hermetic seal.

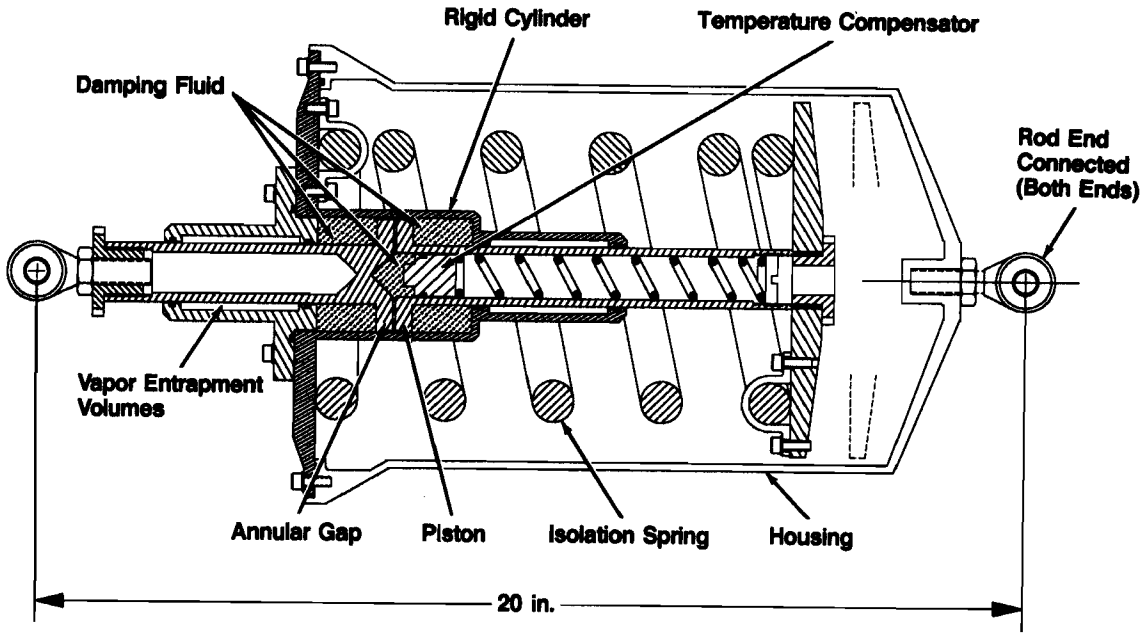

Figure 12. Rigid Volume Damper Isolators

Table 4. Rigid Volume Damper Isolator Specifications

Deflection	±0.91 in.
Velocity	±15 in./s
Damping	35 lb-s/in.
Stiffness	1875 lb/in.
Temperature	
Design	25 ± 5°C
Storage	-35°C to +49°C
Length	20 in. Brg ℄ to Brg ℄
Body Diameter	6.5 in. max
Fatigue Life	Extended
Weight	22 lb

The major features of each type of isolator considered for the SASI application are presented in Table 5. The bellows-type design is superior for on-orbit, small amplitude vibration isolation due to its excellent small displacement (microinch) performance and large dynamic range (five orders of magnitude). The rigid-volume, piston-type isolator has advantages for launch/landing load isolation. Its simplicity, ruggedness, and increased pressure margin make it more economical to manufacture.

Table 5. Isolator Features

Bellows	Piston With Bellows	Piston Without Bellows
• Heritage - Fluidic viscous damping - Hermetic seal - Wide dynamic range - Silicon fluid - Annular flow damper - Pressure preload and Temperature compensation • Lightweight spring	• Heritage - Fluidic viscous damping - Hermetic seal - Silicon fluid - Annular flow damper - Pressure preload and temperature compensation • Lightweight spring • Improved fatigue margin • Reduced fluid leakage potential - Reduced fluid volume - Increased pressure margin - Rugged pressure chamber • Reduced size and weight • Increased adaptability	• Heritage - Fluidic viscous damping - Silicon fluid - Annular flow damper - Pressure preload and temperature compensation • Lightweight spring • Improved fatigue margin • Reduced fluid leakage potential - Reduced fluid volume - Increased pressure margin - Rugged pressure chamber - Redundant seal • Reduced size and weight • Increased adaptability • No offset loading • Rugged design • Improved manufacturability

THE PAYLOAD POINTING SYSTEM ISOLATOR

A study to determine the applicability of the HST viscous damped isolator to the Space Station Payload Pointing System was performed for the Jet Propulsion Laboratory. Such a passive isolation system would probably have cost, reliability, and possibly weight advantages over an active isolation system.

The baseline concept for the study is shown in Figure 13, with eight isolator struts comprising the passive isolation system. Several payloads are planned. However, the study was done using the requirements shown in Figures 14 and 15. These requirements are based on JPL's modelling of the system. The resonant frequency of <0.05 Hz is fundamental for this study. The stroke, damping, and stiffness values K_1 and K_2 are derived from the modelling.

The mass load (1375 pounds) is used as the effective load in the analysis of a single strut. Stiction effects in the end joints can be minimized by using flexure pivots in a two-degree-of-freedom (DOF) gimbal at one end and a three-DOF arrangement at the other.

The appropriate model for a mass-loaded strut is shown in Figure 15; Figure 7 represents the baseline design concept. The spring K_1 represents the stiffness of the bellows (or the parallel spring if it were used). The spring K_2 represents the spring effects in series with the damping element; that is, the compressibility of the fluid and the volume change of the bellows due to the pressure of the fluid. The stiffness ratio will be used in the evaluation of the transmissibility of the isolator strut.

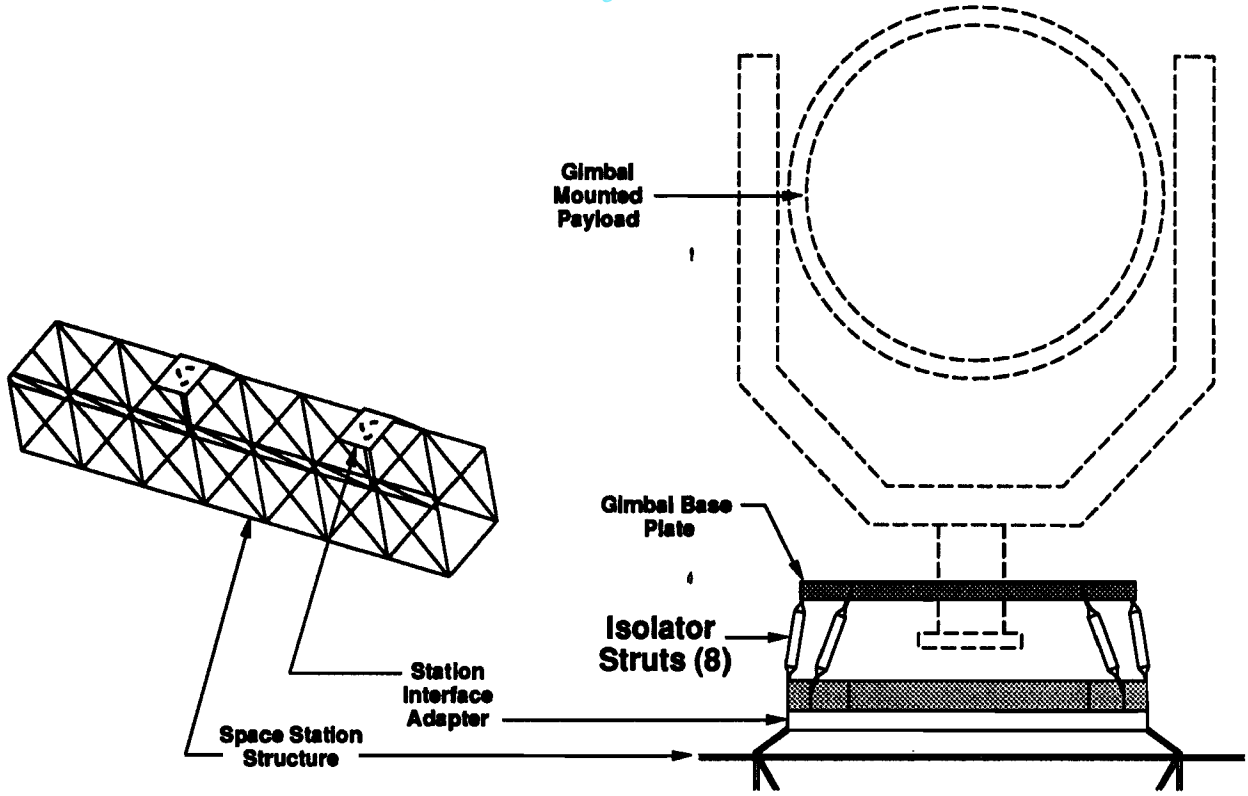

Figure 13. Passive Isolation of Space Station Attached Payload Pointing System

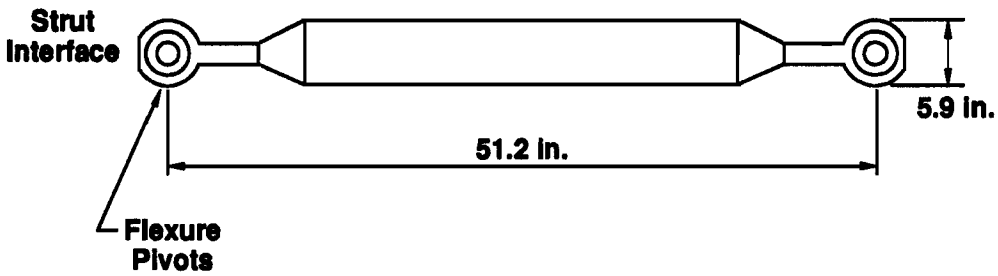

Resonant Frequency	<0.05 Hz
Stroke	±3.15 in.
Effective Mass Load	~1375 lb
Damping	3.4 lb/(in./s)
Stiction	Minimize
Life	>10 years
Linear Performance	µin. range

Figure 14. PPS Strut Specifications Derived from JPL Requirements

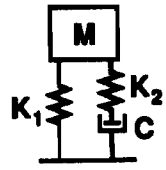

Design	K_1	K_2	C	K_2/K_1
1. SASI Scaled to PPS length	400 lb/in. spring 1.2 lb/in. bellows	3,800 lb/in.	0.26 lb/(in./s)	9.5 3,000
2. SASI Scaled and folded	0.45 lb/in.	1,350 lb/in.	3.4 lb/(in./s)	3,000
3. Design Potential (Double Length, Folded, with Air)	0.22 lb/in.	0.10 lb/in.	3.4 lb/(in./s)	0.5
Requirements	<0.23 lb/in.	<0.70	3.4 lb/(in./s)	—

Figure 15. Summary of Isolator Component Values

An evaluation of the general transfer function was performed to investigate the influence and importance of the various parameters. Figure 16 shows the model and the transfer function of a three-spring isolator and two simplifications of it.

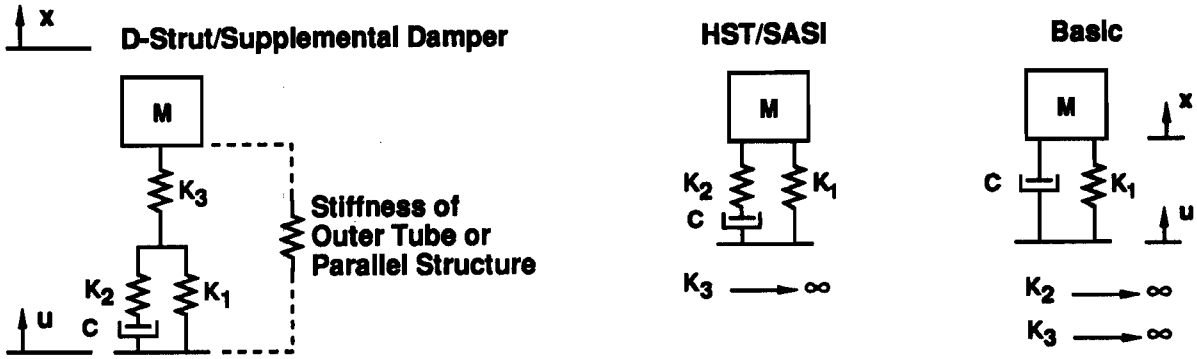

Transfer function

$$\frac{x}{u} = \frac{\frac{B}{Q}\left(1+\frac{1}{N}\right)+1}{\frac{B^3}{QN}\left(\frac{1+N}{P}+1\right)+B^2\left(\frac{1}{P}+1\right)+\frac{B}{Q}\left(\frac{1}{N}+1\right)+1}$$

$$B = \frac{S}{\sqrt{K_1/M}} \qquad Q = \frac{\sqrt{K_1 M}}{C} \qquad N = \frac{K_2}{K_1} \qquad P = \frac{K_3}{K_1}$$

Figure 16. Isolator Modules

The effects of varying the spring values are shown in Figure 17. The curve at the right shows the characteristic for both K_2 and K_3 relatively stiff with respect to K_1(N&P large). Softening K_2 results in the curve that is second from the right; a high frequency isolation increase is seen but with an increased peak just above the break frequency of the basic isolator. Softening K_3, in addition, increases these two effects, as shown by the two left most curves. The middle curve shows the characteristic for a stiff K_2 and a softer K_3. It is shifted left from the baseline curve but shows a smaller peak, more damping, than the other curves. The shift is again due to the lower effective stiffness between the mass and the base. The stronger damping influence is due to the large K_2 imposing larger forces and velocities on the damping element. The roll-off is essentially second order for all curves.

The best combination of isolator elements required for a given application depends on the vibration input, the sensitivity of the isolated body to various frequencies, and the structural characteristics of the body and the base. Figure 5 illustrates this for single-spring isolator. The K_1 value is chosen to set the resonant frequency and then damping is added to reduce the resonant peaking, at some cost to high-frequency isolation. An acceptable balance for the SASI system is shown in Figures 5c and 5f.

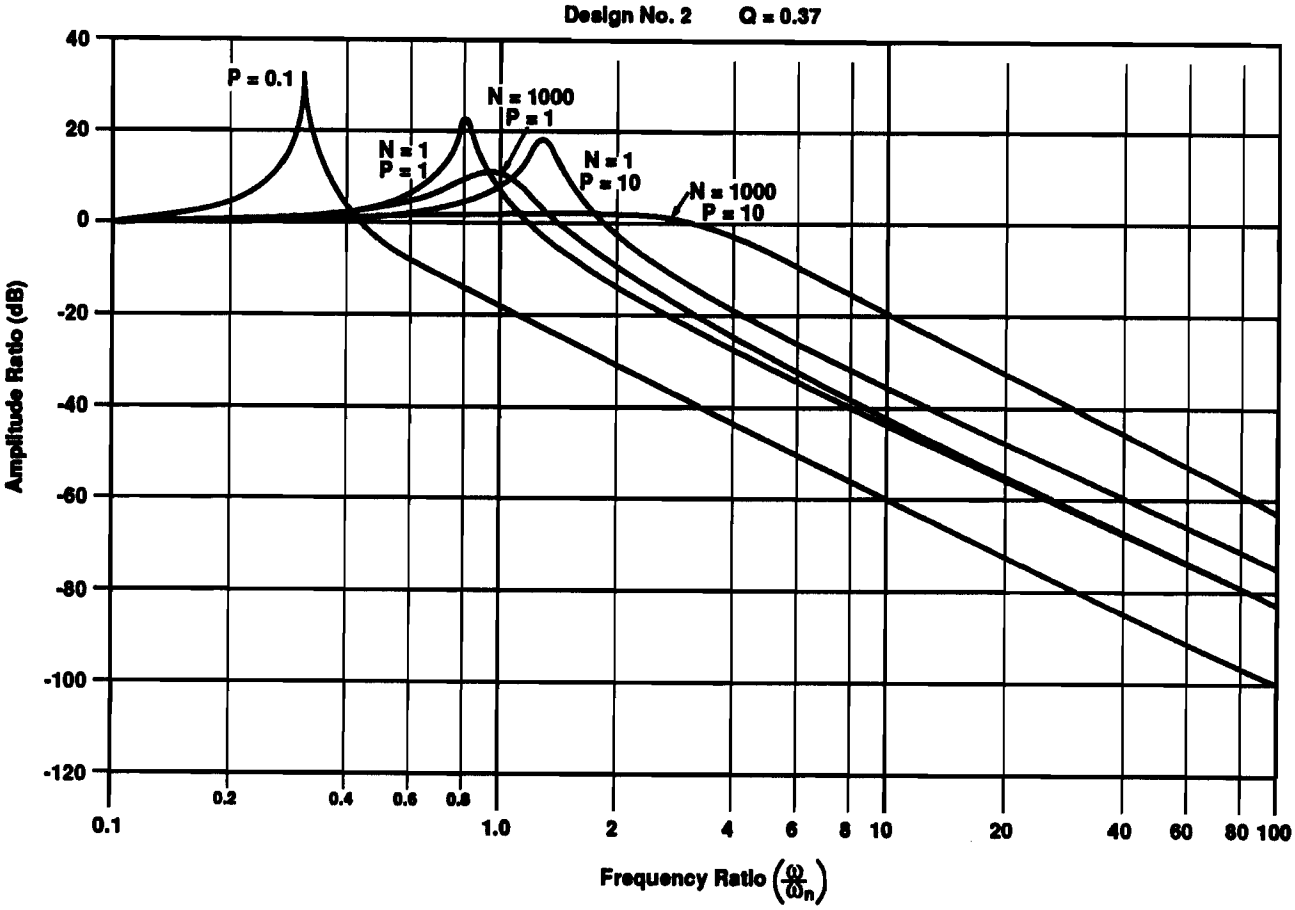

Figure 17. General Isolator Transfer Function

Figure 18 shows the transmissibility for the second design of Figure 15. This design represents the first attempt at meeting the requirements by scaling the SASI design. It is within the length requirement, but the effective bellows length is increased by "folding," that is, arranging the design so that the two active bellows and the compensator bellows are beside each other rather than end to end. The effective length is roughly tripled this way, reducing the bellows stiffness K_1 to one-third. The value for K_1 is still twice the required value; doubling the length would reduce the bellows stiffness, K_1, as needed. The value of K_2 is too large by nearly three orders of magnitude. A means must be used to reduce the effective compressibility of the fluid or effective expandibility of the bellows. Using air changes K_2 by the ratio of the compressibility of silicon damping fluid to that of air. At standard conditions, this ratio is 1/7500. Scaling K_2 by this ratio and doubling the length renders the third design in Figure 15.

Since the damping coefficient depends on the inverse of the radial gap cubed and directly on the viscosity, the damping coefficient can be maintained in spite of the 20:1 viscosity decrease by decreasing the fluid passage radial gap by a factor of about three.

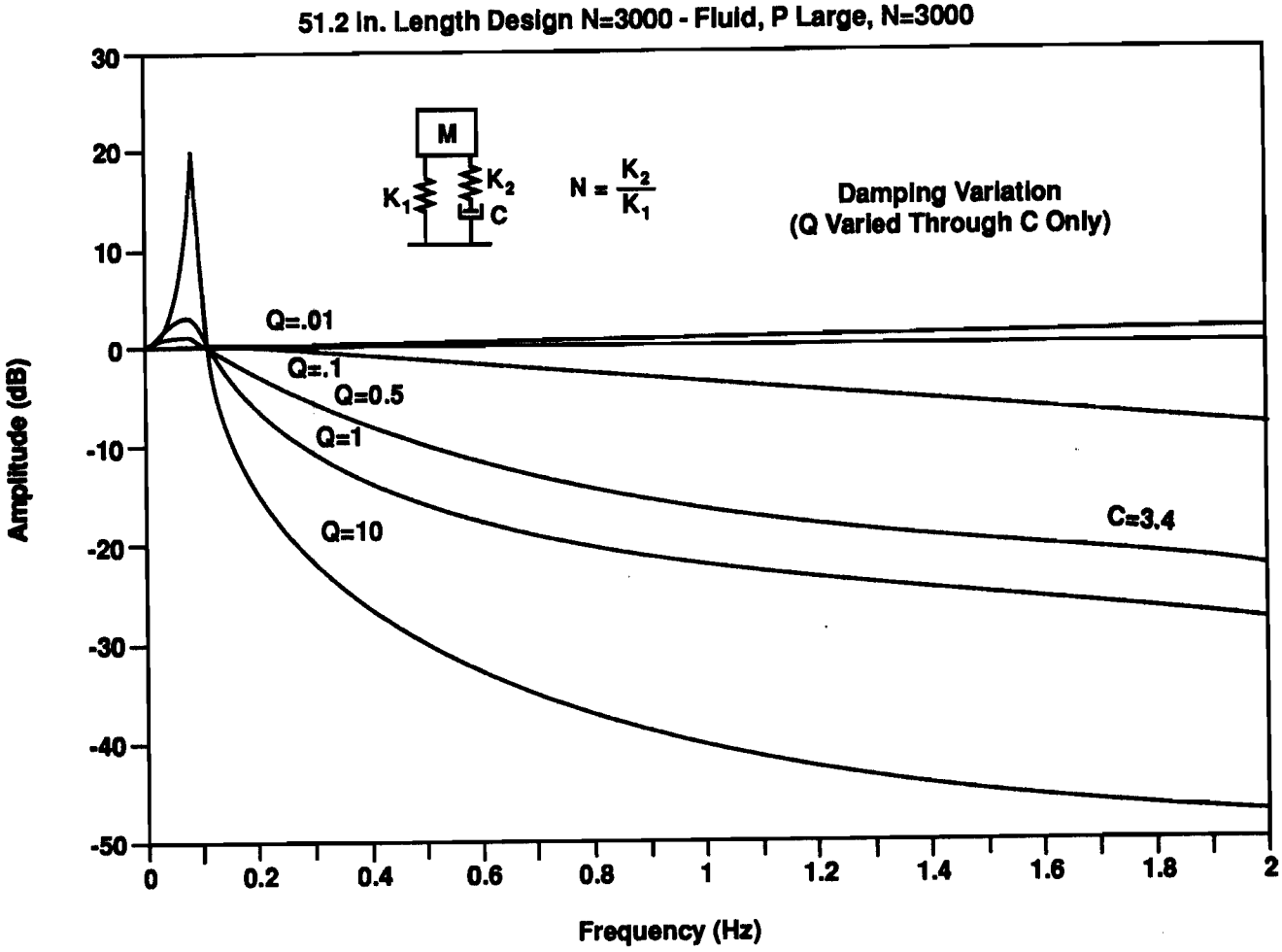

Figure 18. Isolator Transfer Function - Variable Damping

Figure 19 shows the effects on isolation of varying K_2. Note that for a very compressible damping fluid, such as air, high-frequency isolation is improved at the expense of resonant peaking.

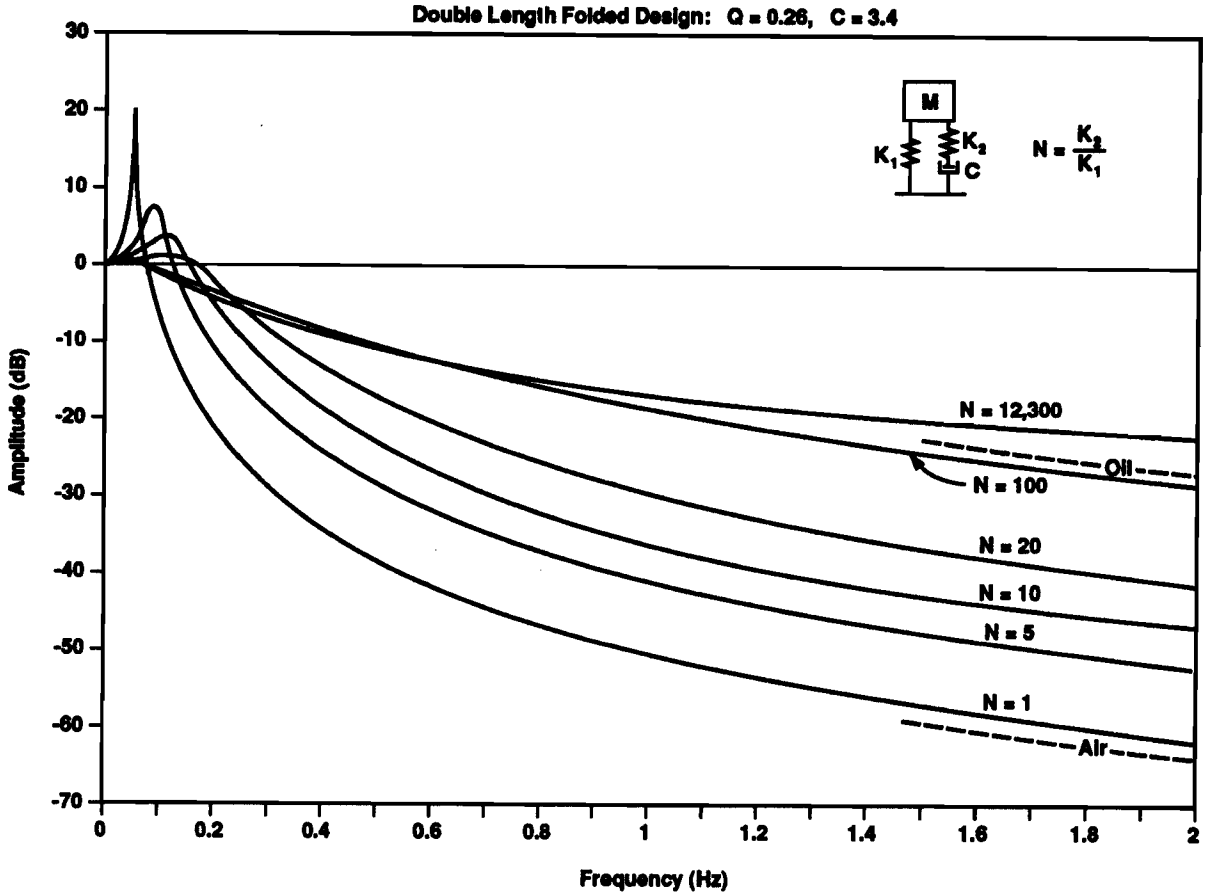

Figure 19. Isolator Transfer Function - Variable K_2

CONCLUSION

This study of an isolator for PPS has shown that the HST concept can be extended to a low stiffness, long stroke application with certain modifications. These include removing the coil spring and using lengthened bellows and a folded design to decrease K_1; air is used as the working fluid to decrease K2. In addition, K3 can be added to also vary the transfer function. In the final PPS isolator system layout and optimization, this versatility can be used to closely obtain the desired isolator strut properties. Some development steps will be necessary to arrive at a flight design. A means must be found to protect the long bellows against buckling (e.g. telescoping concentric tubes) without introducing excess stiction, and tests will be required to verify the damping equations for air.

For isolation of payloads from launch and landing loads, an adaptation of the HST viscous annular flow damping technology, using a high-pressure rigid chamber and piston, has shown to improve manufacturability and reduce weight.

ACKNOWLEDGEMENTS

The following people should be noted for their contributions:

Teresa Hollins; Honeywell Inc., Glendale, AZ
Tom Wilson, Dan Marks, and Dr. Bill Haile; Swales & Associates, Beltsville, MD
Frank Cepallina; Goddard Space Flight Center, Greenbelt, MD
Dr. Ed Wong; Jet Propulsion Laboratory, Pasadena, CA

REFERENCES

Papers:

- Hubble Space Telescope Reaction Wheel Assembly Vibration Isolation System, 1986 Las Vegas Vibration Workshop
- Viscous Damped Space Structure for Reduced Jitter, 1987 58th Shock and Vibration Symposium
- Very High Damping in Large Space Structures, 1987 ASME
- New Structure Design Criteria Offer Improved Pointing and Lower Weight, 1988 59th Shock and Vibration Symposium